Biochemical Journal (2020) **477** 2543–2559
https://doi.org/10.1042/BCJ20200160

PORTLAND PRESS

Research Article

High light induces species specific changes in the membrane lipid composition of *Chlorella*

Janka Widzgowski[1], Alexander Vogel[2], Lena Altrogge[3], Julia Pfaff[2], Heiko Schoof[3], Björn Usadel[1,2], Ladislav Nedbal[1], Ulrich Schurr[1] and Christian Pfaff[1]*

[1]Institute of Bio- and Geosciences (IBG-2: Plant Sciences), Forschungszentrum Jülich, 52425 Jülich, Germany; [2]Institute for Botany and Molecular Genetics, RWTH Aachen University, 52074 Aachen, Germany; [3]Institute of Crop Science and Resource Conservation, INRES Crop Bioinformatics, University of Bonn, 53115 Bonn, Germany

Correspondence: Christian Pfaff (c.pfaff@fz-juelich.de)

Algae have evolved several mechanisms to adjust to changing environmental conditions. To separate from their surroundings, algal cell membranes form a hydrophobic barrier that is critical for life. Thus, it is important to maintain or adjust the physical and biochemical properties of cell membranes which are exposed to environmental factors. Especially glycerolipids of thylakoid membranes, the site of photosynthesis and photoprotection within chloroplasts, are affected by different light conditions. Since little is known about membrane lipid remodeling upon different light treatments, we examined light induced alterations in the glycerolipid composition of the two *Chlorella* species, *C. vulgaris* and *C. sorokiniana*, which differ strongly in their ability to cope with different light intensities. Lipidomic analysis and isotopic labeling experiments revealed differences in the composition of their galactolipid species, although both species likely utilize galactolipid precursors originated from the endoplasmic reticulum. However, *in silico* research of *de novo* sequenced genomes and ortholog mapping of proteins putatively involved in lipid metabolism showed largely conserved lipid biosynthesis pathways suggesting species specific lipid remodeling mechanisms, which possibly have an impact on the response to different light conditions.

Introduction

Algae inhabit very diverse ecosystems from snowfields to desert sand crusts. Their ability to adapt to extreme environmental conditions like salinity, moisture availability, depletion of essential nutrients or changing temperature and light conditions is reflected in their diverse glycerolipid patterns found in their cell membranes. Changing environmental conditions can have an impact on the membrane lipid composition, which can actually have a significant effect on the physical/chemical properties and function of cell membranes. Therefore, lipid metabolism can be used to adjust cell membranes to both gradual and acute stress, enabling the algae to avoid possible impairments [1]. Since light has a strong effect on several metabolic process in phototrophic organisms, exposure to different light conditions can also cause significant changes in the stoichiometry of individual lipid classes and in the composition of fatty acid residues of the respective lipid classes [2,3]. However, little is known about how algal lipid metabolism responds to different light conditions.

The membrane lipid matrix of algae and higher plants is mainly synthesized through the complex interplay of two different pathways located in plastids and the endoplasmic reticulum (ER) [4]. Within plastids, the most abundant glycerolipids are monogalactosyl diacylglycerol (MGDG), digalactosyl diacylglycerol (DGDG), sulfoquinovosyl diacylglycerol (SQDG), and phosphatidylglycerol (PG) which are synthesized via the so-called prokaryotic pathway from phosphatidic acid (PA) and diacylglycerol (DAG). The eukaryotic pathway of glycerolipid synthesis starts with the release of fatty acids from plastids, the activation to acyl-CoA esters, and the export to the ER which ultimately results in the formation of extraplastidic PA and DAG [5]. These extraplastidic glycerolipids are mainly used as

*Present address: PTJ, Forschungszentrum Jülich, 52425 Jülich, Germany.

Received: 2 March 2020
Revised: 16 June 2020
Accepted: 17 June 2020

Accepted Manuscript online: 18 June 2020
Version of Record published: 10 July 2020

Biochemical Journal (2020) 477 2543–2559
https://doi.org/10.1042/BCJ20200160

intermediates for the synthesis of phosphatidylcholine (PC), phosphatidylethanolamine (PE) and some other phospholipids. In many plants a proportion of PA, PC or DAG is re-imported into the plastid to provide ER-derived precursors for eukaryotic galactolipid synthesis [6–8]. In plants, prokaryotic and eukaryotic galactolipids are distinguishable by their fatty acids linked to the sn-2 position because of the different substrate specificities of plastid and ER localized lysophospholipid acyltransferases [9]. Glycerolipids originating from the plastid or the ER synthesis pathways result in the inclusion of C-16 or C-18 acyl chains at the sn-2 position, respectively, while in both pathways C-18 acyl chains are more frequently linked to the sn-1 position [10]. Therefore, only ER-pathway derived galactolipids can exhibit C-18 fatty acids at both positions. Based on the composition of galactolipid precursors, algae and higher plants can be divided into three groups. The first group involves both the plastidial and the ER pathway for galactolipid synthesis while the second group mainly employs the eukaryotic pathway. The third group, including most green algae, synthesizes galactolipid molecular species comparable to those exclusively derived from the plastidial pathway [11]. Unlike higher plants, the green algae *Chlamydomonas reinhardtii* has a distinct ER localized lysophosphatidic acid acyltransferase (LPAAT) with prokaryotic substrate preference and thus synthesizes 'prokaryotic' lipid molecular species within the ER [12]. Therefore, it is so far unclear if *Chlorella* also utilizes the eukaryotic pathway for the synthesis of galactolipids.

The composition of galactolipid species and the ratio of MGDG:DGDG is known to influence the properties of chloroplast membranes [13]. It has been reported that several algal genera show light induced alterations in their total fatty acid profiles and changes in their MGDG:DGDG ratio, whereas little is known about the interplay of the prokaryotic and the eukaryotic pathway and its role of galactolipid remodeling under different light regimes. Therefore, we selected two different species of the *Chlorella*-clade belonging to the *C. vulgaris* and the *C. sorokiniana* linage to further investigate the role of lipid remodeling under different light regimes of coccoid green algae [14,15]. These freshwater algae are unicellular, immobile and asexual organisms with simple morphology and non-complex chloroplasts but show comparable lipid profiles to those of higher plants. Cell membranes of *Chlorella* are mainly comprised of the galactolipids MGDG and DGDG while ∼15% of their membranes are build up of the phospholipids PC and PE.

By analysis of lipid molecular species and ^{14}C-labeling experiments, we observed that both species involve the ER pathway for galactolipid synthesis with clear differences in their galactolipid molecular species composition. Based on the profiles of membrane lipids and genome sequencing followed by *in silico* analysis of genes putatively involved in *Chlorella* lipid metabolism, we illustrate light induced remodeling of membrane lipids in two different *Chlorella* species. Our results show that both *Chlorella* species use different precursors for galactolipid synthesis which are possibly involved in the response to different light conditions.

Experimental procedures

Algal strains and cultivation conditions

The *Chlorella* species *C. sorokiniana* 211-8k and *C. vulgaris* 211-11b were obtained from SAG (Göttingen, Germany). Axenic algal cultures were grown in TAP medium [16] on an orbital shaker at 120 rpm, 30°C and a photon flux density of 250 μmol m^{-2} s^{-1} or 1000 μmol m^{-2} s^{-1} using a 16 h light/8 h dark cycle. The algal cells were sampled during their late exponential growth phase. Photoorganothrophic conditions were used to overcome pure self-shading effects of freshly inoculated cultures.

Phylogenetic analysis

Sequence alignments of 18S RNA, ITS1, and ITS2 were constructed in MEGA7 using Muscle then the Maximum Likelihood tree was generated [17]. The supporting bootstrap values correspond to Maximum Likelihood (ML) and Neighbor Joining (NJ) and were performed with 1000 replications.

Determination of photopigment contents

Liquid *Chlorella* cultures (10 ml) were harvested, washed with water, and immediately re-suspended in 1 ml ice cold extraction solution (acetone:water (80 : 20; v/v) with 5% $CaCO_3$ (v/v)). An equal volume of precooled ceramic beads (3.0–3.3 mm diameter; Soilgene) were added and cells were disrupted by vortexing for 5 min. The extracts were then transferred into a 2 ml tube to remove cell debris by centrifugation (5 min, 20 000×***g***, 4° C). Since matrix effects occurred in the pigment extracts, we extracted them three times with 5 ml cold petroleum ether. The pigment containing organic phases were allowed to evaporate until near dryness under a

stream of nitrogen gas, and the residues were dissolved in methanol. In order to verify that all pigments were quantitatively extracted from the aqueous phase, we removed the water by freeze drying and dissolved the residues in methanol.

Immediately after extraction all samples were analyzed by HPLC using an Agilent 1260 system equipped with a photodiode array detector. The reverse-phase system consisted of a ProtoSil C30 column (250 × 4.6 mm, 3 μm; Bischoff, Germany) which was developed at 20°C (column oven temperature) with a gradient (flow rate of 0.5 ml min^{-1}) of solvent B (2-methoxy-2-methylpropane) in solvent A (methanol : water (99.3 : 0.7; v/v), 1 mM ammonium ethanoate). The analysis of pigments with isocratic elution steps was performed as follows (all v/v): A:B (85 : 15) to A:B (70 : 30) and kept for 6 min; A:B (70 : 30) to A : B (15 : 85) in 5 min and kept for 7 min; A : B (15 : 85) to A : B (85 : 15) in 5 min and kept for 5 min. The detection was carried out at a wavelength of 440 nm, absorption spectra were measured between 260 nm and 600 nm and the data were extracted and analyzed using MassHunter software (Agilent) by comparing retention time and absorption spectra of standard compounds.

Measurement of oxygen evolution

Chlorella cells were re-suspended in 1 ml TP medium to a final OD_{735} of 0.2. $NaHCO_3$ (3 mM final concentration) was added to cell suspensions prior to O_2 evolution measurements to ensure sufficient carbon supply. The cell suspensions were then transferred into a liquid phase oxygen electrode chamber (Hansatech) and exposed to 50 μmol m^{-2} s^{-1} or 1000 μmol m^{-2} s^{-1} at 30°C.

Lipid extraction

Chlorella liquid cultures (50 ml) were harvested by centrifugation, washed with cold water, re-suspended in 1 ml water and transferred into a glass grinding tube. Equal volumes of ceramic beads (3.0–3.3 mm diameter; Soilgene, Germany) and 7.5 ml of precooled chloroform/methanol (2 : 1; v/v) were added for extraction [18]. Cells were disrupted by vortexing for 5 min followed by the addition of 2.5 ml 0.9% NaCl solution and centrifugation for 5 min, 3000***g*** at room temperature. After phase separation, the chloroform phase was collected and the aqueous phase was re-extracted twice with 3 ml chloroform. The combined chloroform phases were dried under a stream of nitrogen gas, dissolved in chloroform/methanol (2 : 1; v/v) and stored in amber glass with protected gas (Ar) at −20°C. All extraction steps were performed in acetone cleaned glassware.

Fatty acid analysis

Lipid extracts were dried under a stream of nitrogen gas, solved, and transmethylated in 2 ml 0.5 M sulphuric acid in methanol with dimethoxypropane (2%; v/v) for 1 h at 80°C with 250 nmol heptadecanoic methyl ester and 250 nmol pentadecanoic as internal standards. Fatty acid methyl esters were extracted with 3 ml n-heptane on a shaker at room temperature for 2 h [19] and analyzed by GC-MS (Agilent 7890A) with an Optima 5 MS column (30 m × 0.25 mm, 0.25 μm film thickness; Macherey & Nagel) using He as carrier gas with constant flow (1 ml/min). Samples were split injected (1 : 10) and subjected to the following temperature program: Initial hold at 120°C for 2 min; 10°C/min ramp to 150°C; 0.5°C/min ramp to 172.5°C and held for 10 min; 0.5°C/min ramp to 172.7°C/min; 10°C/min ramp to 270°C and held for 1 min. Fatty acid methyl esters were identified by retention times and m/z using chemstation (Agilent) software.

Membrane lipid analysis

The composition of glycerolipids (MGDG, DGDG, SQDG, PA, PC, PE, PG, PI, and PS) was analyzed by direct infusion tandem mass spectrometry as described in [20] with minor modifications.

With regard to the sample concentration, an aliquot of each lipid extract was diluted in methanol/chloroform/300 mM ammonium acetate (665 : 300 : 35, v/v) [21]. Two internal phospholipid standards each were added for PC, PE, PG, PA, PS, and PI (Avanti Polar Lipids) in a final concentration of 1 μM. The galactolipid standards MGDG, DGDG, and SQDG (Avanti Polar Lipids and Matreya LLC) were hydrogenated for 6 h at 25°C in aceton/methanol (1 : 1) using 1% Pt(IV)oxide (w/w) and >1 atm H_2 and used in a final concentration of 10 μM [22]. Samples were measured with a triple quatrupole mass spectrometer (ESI-MS/MS) (6420, Agilent) using constant injection of a PSD/3 syringe pump (Hamilton) with flow rate of 6 μl min^{-1}. Each lipid class was measured for one minute with specific settings shown in Supplementary Table S10. After correction of isotopic overlap, lipid molecular species were quantified as described in [23].

Biochemical Journal (2020) 477 2543–2559
https://doi.org/10.1042/BCJ20200160

Positional analysis

Lipid extracts were evaporated under a stream of nitrogen gas and mixed with 2 ml 40 mM Tris-HCl (pH 7.2) buffer containing 50 mM Na_3BO_3 and 150 U lipase of *Rhizopus oryzae*. The mixture was incubated in a ultrasonic bath for 2 h at 22°C [24]. After extraction with chloroform/methanol (2 : 1; v/v) the lyso-glycerolipids (lyso-MGDG, lyso-DGDG, lyso-PC, lyso-PE, lyso-PG) were analyzed by direct infusion tandem mass spectrometry as stated above.

Isotopic labeling with acyl-CoA

Chlorella cultures were grown in TAP medium (25 ml) to an OD_{735} of 0.5 and were then incubated with 4 μCi of Palmitoyl [1-^{14}C] Coenzyme A or Oleoyl [1-^{14}C] Coenzyme A for another 2 days. Cells were harvested, washed with water, and lipids were extracted as stated above. The lipid extracts were separated by TLC, developed in chloroform/methanol/acetic acid/water (90 : 31 : 4 : 4; v/v), and radioactively labeled compounds were visualized with a FLA-3000 bioimager (Raytest).

DNA extraction

Late exponential *Chlorella* was harvested from liquid culture (100 ml, $OD_{735} > 2.0$) by centrifugation for 10 min at 10 000×***g*** and 4°C and the cell pellet was re-suspended in 2 ml water and 4 ml extraction buffer (100 mM Tris-HCl, 150 mM NaCl, 5 mM dithiothreitol, 1% L-lauroylsarcosine). Approximately 3 ml ceramic beads (3.0–3.3 mm diameter; Soilgene, Germany) were added and cells were disrupted by vortexing for 5 to 10 min. Subsequently, the liquid phase was transferred to another tube, and cell debris was removed by centrifugation for 10 min at 10 000×***g*** and 4°C. The sample was extracted with 3 ml chloroform/3-methylbutan-1-ol (24 : 1; v/v) and 3 ml phenol by 15-time inverting of the sample tube. The aqueous phase was separated by centrifugation (10 min, 10 000×***g***, 4 °C), transferred to another tube, acetified with 400 μl Na-acetate (pH 5.2) and total DNA was precipitated with 1.5 vol. 2-propanol at 4°C for 20 min. After centrifugation, the DNA pellet was washed with 70% ethanol (v/v) and re-suspended in water. The DNA was treated with RNase (Thermo Fisher) and used for genome sequencing.

Short-read genome sequencing and assembly

De novo whole genome sequencing for all strains was performed following the Illumina TruSeq PCR-free library preparation protocol and sequencing on an Illumina MiSeq platform (MCS 2.5.0.5, RTA 1.18.54) with 600v3 chemistry. Following initial data quality control using FastQC, adapter sequences and low quality bases were removed using Trimmomatic v0.35 [25]. SPAdes (v3.6.2) was used for contig and scaffold assembly of the paired-end Illumina data without previous error correction [26]. Resulting scaffolds were blasted against the NCBI nucleotide database and scaffolds with a hit to PhiX were removed from the assembly [27].

Long-read nanopore library preparation, sequencing and assembly

A modified library preparation protocol was used to enable enrichment of large fragments of either >20 kb or >40 kb with a Blue Pippin device. For all libraries prepared with R7.3 chemistry, size selection was performed after end-repair and adenylation, while in R9.4 libraries large fragments were enriched directly after fragmentation. All generated sequences were converted to fastq-format using poretools v0.5.1 [28] and redundant reads were removed based on 1D/2D classification or length filtering.

Additionally, *de novo* assembly of the nanopore longreads was performed with Canu (version1.3+, commit b147f45b), with the following non-default parameters (corOutCoverage = 5000, corMinCoverage = 0) and two rounds of error correction [29]. The raw assembly was then polished in four iterations of pilon polishing with the available trimmed Illumina data [30]. Nanopolish v0.6.1 was used to predict 5-mC modification from the R9.4 nanopore reads of library Cs8k 003 003 aligned to the four time pilon polished canu assembly [31]. For comparison, hybrid assemblies were generated using SPAdes v3.9.0 [26].

Genome size estimation

Genome sizes were estimated by generating and counting 17-mers from the trimmed short-read data using Jellyfish (v2.2.4) and GCE (v1.0.0) [32,33].

Biochemical Journal (2020) 477 2543–2559
https://doi.org/10.1042/BCJ20200160

Chloroplast comparison

For identification of chloroplast scaffolds, all scaffolds for the final assemblies were blasted against the NCBI nucleotide database (2016-03-29). Resulting scaffolds were aligned against the published *C. sorokiniana* 211-8k chloroplast genome [34] using LAST (v712) and suggested settings for strongly similar genomes [35].

RNA extraction and sequencing

RNA was isolated using MasterPure Plant RNA Purification Kit (Epicentre, USA) with few modifications. Three independent biological replicates of *Chlorella* liquid cultures (50 ml) were harvested by centrifugation (10 000×***g***, 10 min, 4°C) and the pellets were immediately flash frozen with liquid nitrogen. The samples were re-suspended in plant tissue and cell lysis solution containing 1 mM dithiothreitol and 100 μg Proteinase K and incubated at 56°C for 30 min. The nucleic acids were precipitated with 800 μl 2-propanol and washed with 70% ethanol (v/v). The RNA was treated with DNase I solution (RNase free DNase I 5 U/sample) and incubated at 37°C for 30 min. For sequencing the RNA samples were washed again with 70% ethanol (v/v) and dissolved in 20 μl RNase free water. Quantity was checked via Qubit and quality control was performed by agarose gel electrophoresis.

Library preparation was performed by the supplier using the Kapa Stranded mRNA-Seq Kit and sequencing was performed on a HiSeq Illumina system (DNA Sequencing Center, Brigham Young University, Provo, U.S.A.).

Gene annotation

Paired-end raw RNA-seq reads were quality trimmed with Trimmomatic v0.36 [25] and mapped to the assemblies using Bowtie2 v2.5.0 [36] and TopHat2 v2.2.1 [37]. Duplicate reads were removed with the PICARD MarkDuplicates tool v2.5.0 [38]. The genome assemblies were repeat-masked using RepeatMasker v4.0.6 [39] with the species option 'chlorellales' and annotated with the BRAKER1 v1.9 [40] genome annotation pipeline. Orthologous groups of predicted genes were identified using OrthoFinder [41] and sequence similarity searches were carried out with BLAST v2.3.0+ [27] in the UniProtKB/Swiss- Prot (2016-06) and TAIR 10 (2012-04-16) databases. Human Readable Descriptions (HRD) and Gene Ontology (GO) terms were assigned to predicted genes using AHRD v3.3 [42] provided with a reference UniProtKB Gene Ontology Annotation (GOA) file (2016-07-06). Genome Annotation Completeness was assessed with BUSCO v2.0 [43] using the lineage-specific BUSCO dataset for chlorophyta.

In silico analysis of glycerolipid metabolism

The prediction of proteins involved in glycerolipid metabolism was performed using blast+ [32] searches against reference sequences using databases of *A. thaliana*, *C. reinhardtii*, *Saccharomyces cerevisiae*, cyanobacteria and some other bacteria [5,44–47]. Both, the genome sequences and the *ab initio* predicted gene models of *C. vulgaris* 211-11b and *C. sorokiniana* 211-8k were used to find orthologs with an E-value of $<e^{-30}$.

Results

Phylogenetic analysis

To investigate the impact of different light conditions on the glycerolipid metabolism, we selected two *Chlorella* species. *C. sorokiniana* 211-8k was isolated in subtropical climate (Austin, USA) and was compared to the eponymous species of the genus *Chlorella*, *C. vulgaris* 211-11b, isolated in Delft, Netherlands [16,17]. Based on 18S rRNA/ITS1-2 both species were assigned into the *Chlorella* clade (Figure 1) as also described in Bock et al. [48].

Light induced changes in growth, photopigment composition and oxygen evolution

In order to identify growth characteristics, *C. vulgaris* and *C. sorokiniana* were cultivated at 30°C and 50 μmol photons m^{-2} s^{-1} (low light, LL) or 1000 μmol photons m^{-2} s^{-1} (high light, HL). The growth curves of batch cultivated *C. vulgaris* showed significant growth reduction under high light condition whereas *C. sorokiniana* grew best under the same light treatment (Figure 2).

To examine the adaptation to different light conditions, we analyzed the light-dependent xanthophyll conversion of the two *Chlorella* species. The reversible conversion of violaxanthin to zeaxanthin via the intermediate antheraxanthin is an important strategy of many plants and algae to avoid or minimize damage related to light-induced photo-oxidative stress [49]. As shown in Figure 3a,b, both species responded to high light

Biochemical Journal (2020) 477 2543–2559
https://doi.org/10.1042/BCJ20200160

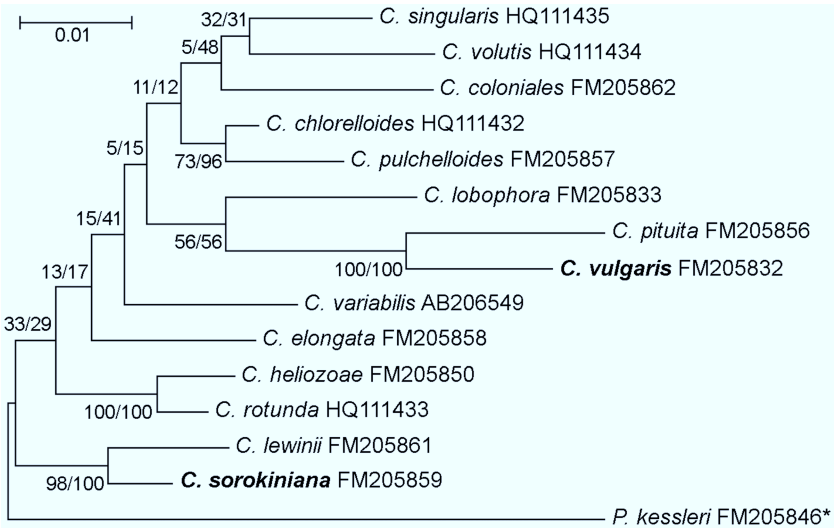

Figure 1. *Chlorella* phylogeny.

For the phylogenetic tree, sequence alignments (18S RNA, ITS1, and ITS2) were constructed in MEGA7 using Muscle then the Maximum likelihood tree was generated [17]. The supporting bootstrap values correspond to Maximum Likelihood (ML) and Neighbor Joining (NJ) (ML/NJ) and were performed with 1000 replications. *Parachlorella kessleri* was used as outgroup. The scale bar represents 0.01 nucleotide substitutions/site.

treatment with significant shifts in their xanthophyll composition. The increase of de-epoxidized xanthophyll cycle compounds (antheraxanthin and zeaxanthin) caused by high light treatment is commonly accepted as a pivotal photoprotection mechanism [49] which can be described as the de-epoxidation state (DES). *C. sorokiniana* exhibited a DES value of 21% under low light conditions and 42% under high light conditions, respectively. *C. vulgaris* showed DES values within a similar range (16%, low light; 49%, high light) (Figure 3e). These results indicate a comparable photoprotection mediated by the de-epoxidation of xanthophylls between both species. However, *C. vulgaris* responded to high light treatment with a threefold decrease in the total pigment content with the most significant decrease in chlorophyll a and chlorophyll b amounts while the total pigment content of *C. sorokiniana* remained constant (Figure 3a–d and Supplementary Table S1). Particularly, the xanthophyll-pool size of low light cultivated *C. vulgaris* remained constant under both light treatments. In contrast, the xanthophyll-pool size of low light treated *C. sorokiniana* was less than half of *C. vulgaris* but its pool

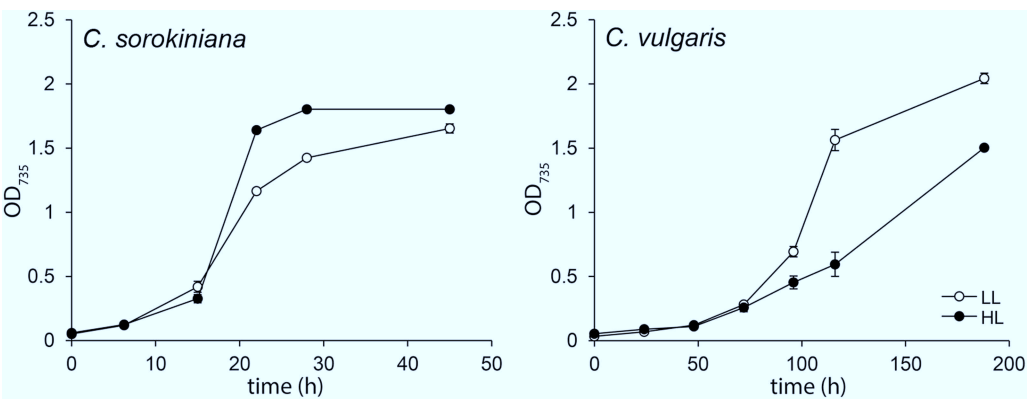

Figure 2. Light dependent growth of two *Chlorella* strains.

Chlorella strains were batch cultivated in TAP medium at 30°C and 50 μmol photons m^{-2} s^{-1} (LL, low light) or 1000 μmol photons m^{-2} s^{-1} (HL, high light) using a 16 h light/ 8 h dark cycle. Progress of cell growth was determined by measuring the increase of OD_{735}. The values are the means with the respective standard deviation ($n = 3$ biological replicates).

Biochemical Journal (2020) 477 2543–2559
https://doi.org/10.1042/BCJ20200160

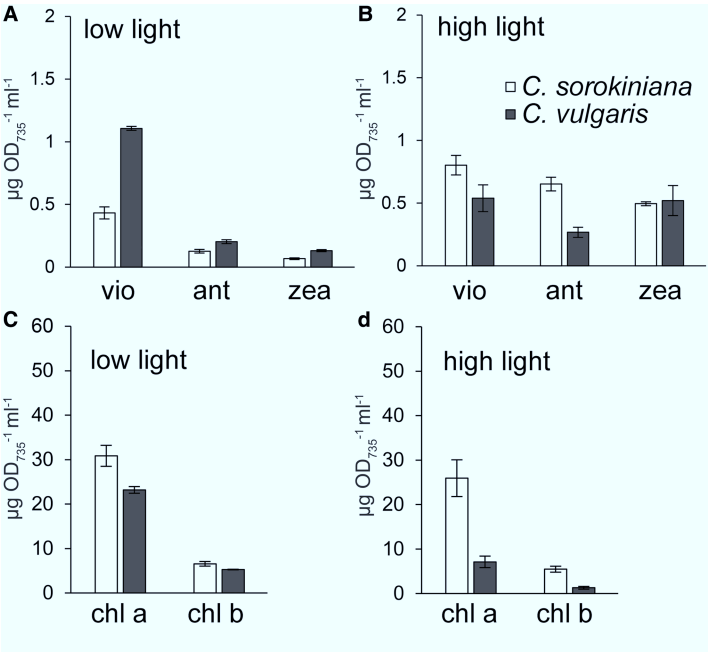

e

	C. sorokiniana		*C. vulgaris*	
	LL	HL	LL	HL
DES [%]	21 ± 1	42 ± 1	16 ± 1	49 ± 7
Σ Pig. [µg OD_{735}^{-1} ml^{-1}]	42.31 ± 3.27	39.56 ± 5.61	33.20 ± 0.89	12.11 ± 2.12
Σ Xan. [µg OD_{735}^{-1} ml^{-1}]	0.63 ± 0.07	1.95 ± 0.18	1.44 ± 0.02	1.33 ± 0.23
O_2 [µmol mg Chl^{-1} h^{-1}]	122.6 ± 0.87	277.4 ± 1.21	112.2 ± 0.81	113.6 ± 1.49

Figure 3. Light induced changes in photopigment composition and oxygen evolution.
Xanthophylls (**a**,**b**) (violaxanthin (vio), antheraxanthin (ant), zeaxanthin (zea)), and chlorophylls (**c**,**d**) (chlorophyll a (chl a), chlorophyll b (chl b)) were analyzed by high-performance liquid chromatography (HPLC) of low light (LL; 50 µmol photons m^{-2} s^{-1}) and high light (HL; 1000 µmol photons m^{-2} s^{-1}) treated *Chlorella* cells, which were harvested in the late exponential growth phase. (**e**), The de-epoxidation state (DES) (DES = (zea + 0.5ant)/(vio + ant + zea)), total pigment amounts (Σ Pig.) and xanthophylls pool size (Σ Xan.) were calculated from data shown in Supplementary Table S1. Oxygen evolution was measured with a liquid phase oxygen electrode chamber. The values are the means with the respective standard deviation ($n = 3$ biological replicates).

size increased approximately three times under high light conditions. In addition, oxygen evolution rates of high light treated *C. sorokiniana* were more than twice as high as the photosynthetic activity of low light cultivated cells. The oxygen evolution rates of *C. vulgaris* were comparable under both light conditions and with this comparable to the oxygen evolution rate of low light treated C. sorokiniana (Figure 3e). These results show that xanthophyll de-epoxidation is comparable in both strains. But the remarkable differences in high light induces growth behavior, pigment degradation, xanthophyll pool size and oxygen evolution suggests that *C. vulgaris* and *C. sorokiniana* posses different adaptation mechanisms to the tested light conditions.

Inventory of *Chlorella* glycerolipids

To investigated light induced alterations within the membrane lipid composition we analyzed *Chlorella* lipid classes and lipid molecular species. Relative quantification of the main glycerolipid classes revealed highest amounts of the galactolipids MGDG and DGDG in both *Chlorella* species. Much smaller amounts of the phospholipids PC, PE, PG, and PA were measured while PI, PS, and the sulfolipid SQDG were close to the detection limit (Figure 5a). The betain lipid diacylglyceryl-N,N,N-trimethylhomoserine (DGTS) and its precursor diacylglycerylhomoserine (DGHS) were not detectable under the tested conditions. The fatty acid composition of *Chlorella* membrane lipids largely consists of C-16 and C-18 acyl chains with 0, 1, 2 or 3 double bonds

Biochemical Journal (2020) 477 2543–2559
https://doi.org/10.1042/BCJ20200160

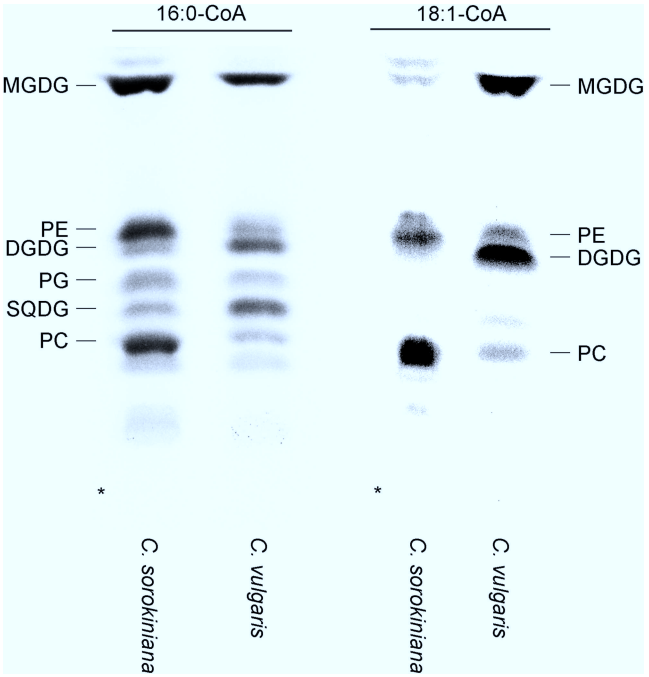

Figure 4. Isotopic labeling of glycerolipids with [1-^{14}C]16:0-CoA and [1-^{14}C]18:1-CoA.

C. sorokiniana and *C. vulgaris* were incubated for 3 days with [1-^{14}C]16:0-CoA and [1-^{14}C]18:1-CoA at 30°C and 50 μmol photons m^{-2} s^{-1}. Their lipid extracts were separated by TLC and radioactively labeled compounds were detected with a bioimager (Raytest). *, origin.

(Supplementary Figure S1). Analysis of the fatty acids linked to the respective lipid classes showed a very similar composition of phospholipid molecular species of the two algal strains (Figure 5b). In contrast, differences were observed in their galactolipid molecular species. In particular, *C. vulgaris* possessed galactolipids with two C-18 acyl chains (36:X) while *C. sorokiniana* exhibited mainly 34:X species, which was confirmed by positional distribution analysis of glycerolipids (Table 1). Furthermore, analysis showed only C-16 acyl chains at the sn-2 position in *C. sorokiniana*, assuming the production of galactolipids exclusively via the plastidial pathway, while *C. vulgaris* probably employs the plastidial and the ER pathway, as positional analysis exhibited also 18 : X species at the sn-2 position (Table 1). But isotopic labeling experiments with [1-^{14}C]16 : 0-CoA showed its incorporation into phospholipids and galactolipids which clearly suggests the synthesis of galactolipids from eukaryotic precursors in both species (Figure 4). When [1-^{14}C]18 : 1-CoA was applied as substrate, in *C. sorokiniana* the incorporated radioactivity was largely observed in the phospholipids PC and PE whereas hardly any radioactivity was detectable in MGDG and DGDG, while *C.vulgaris* accumulated major amounts of isotopic labeled galactolipids. Hence, both species possess galactolipids from ER-derived precursors although galactolipid molecular species of *C. sorokiniana* look like exclusively plastid-derived.

Glycerolipid composition under different light conditions

High light treatment caused species specific alterations in the composition of membrane lipids with largest differences in the amounts of galactolipids (Figure 5a). In particular, *C. vulgaris* turned its MGDG : DGDG ratio from approximately 3 : 1 to 1 : 2, whereas *C. sorokiniana* decreased its ratio from approximately 7 : 1 to 5 : 1. Furthermore, *C. vulgaris* responded to high light with a strong increase of PA and PC and a decrease in PG while the relative amounts of phospholipids of *C. sorokiniana* were less affected by high light.

Comparison of high light induced alterations in lipid molecular species revealed a highly similar shift in PG molecular species, suggesting not only a general role of PG in photosynthesis [50] but also a specific role of the different PG molecular species. In contrast, molecular species of PC and PE with two C-18 acyl chains were only increased in *C. vulgaris* which might also be related to the high light induced increase of 36 : X galactolipid molecular species (Figure 5b). Thus, high light treated *C. vulgaris* showed significant changes in almost all

Biochemical Journal (2020) **477** 2543–2559
https://doi.org/10.1042/BCJ20200160

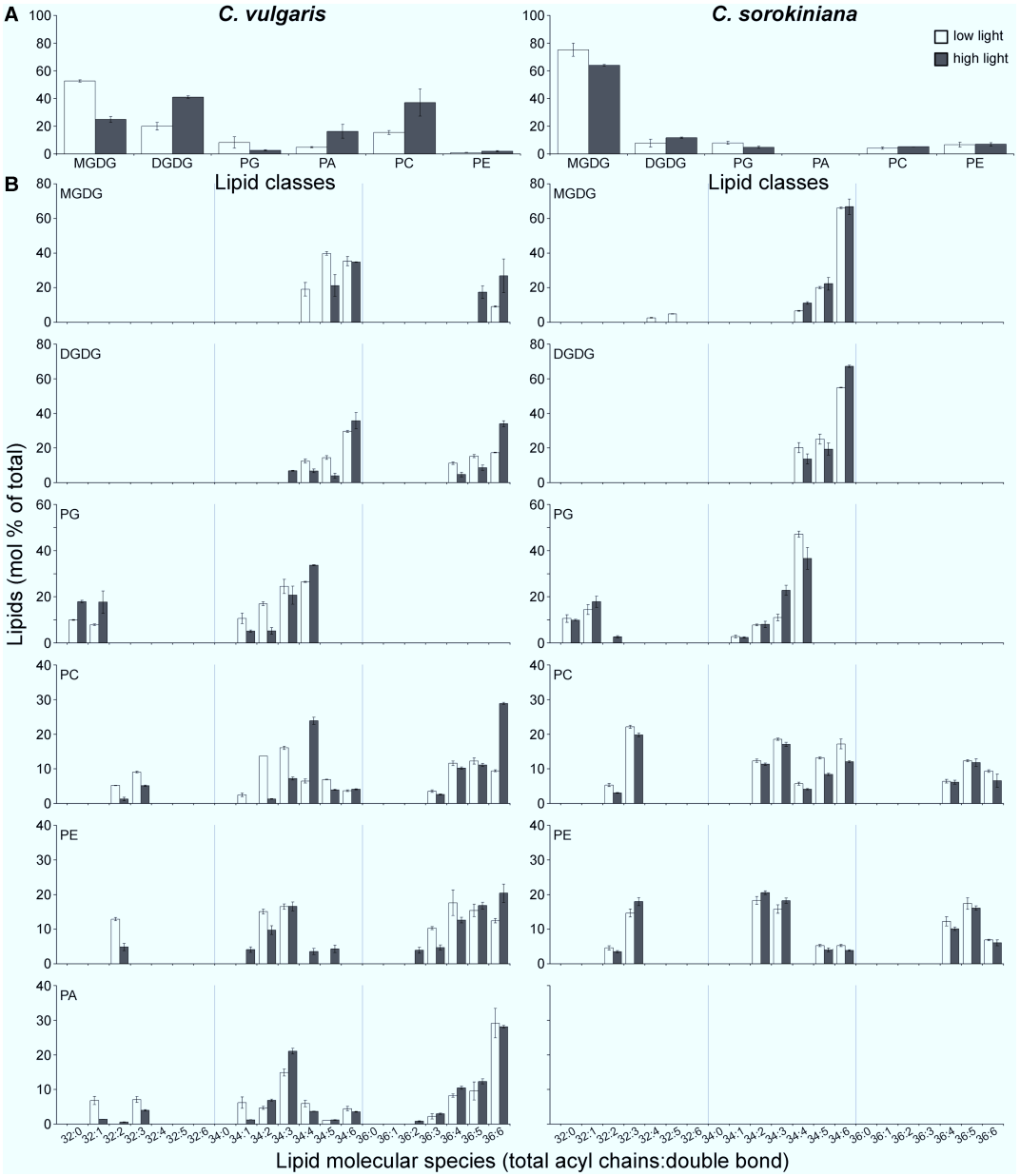

Figure 5. Light induced changes in lipid classes and lipid molecular species.

Lipid classes (**a**) and lipid molecular species (**b**) were analyzed by direct infusion tandem mass spectrometry of low light (50 μmol photons m^{-2} s^{-1}) and high light (1000 μmol photons m^{-2} s^{-1}) treated *Chlorella* cells which were harvested in the late exponential growth phase. The values are the means with the respective standard deviation ($n = 3$ biological replicates). Abbreviations: DGDG, digalactosyldiacylglycerol; MGDG, monogalactosyldiacylglycerol; PA, phosphatidic acid; PC, phosphatidylcholine; PE, phosphatidylethanolamine; PG, phosphatidylglycerol.

glycerolipid classes and numerous lipid molecular species, while *C. sorokiniana* showed distinctly smaller alterations. It is worth noting that some differences between the two species are already apparent at low light conditions, such as galactolipids with two C-18 acyl chains. Therefore, by sequencing and analyzing their genomes, we reconstruct the putative lipid metabolism of *C. vulgaris* and *C. sorokiniana* in order to uncover differences in glycerolipid biosynthesis which are possibly involved in light induced changes in the glycerolipid composition.

Biochemical Journal (2020) 477 2543–2559
https://doi.org/10.1042/BCJ20200160

Table 1 Positional distribution of fatty acids on *Chlorella* glycerolipids

	C. sorokiniana 211-8k		*C. vulgaris* 211-11b	
	Sn-1[1]	sn-2	sn-1[2]	sn-2
MGDG	- 18:2–3	16:1–3 -	16:X 18:2–3	16:1–3 18:1–3
DGDG	- 18:2–3	16:1–3 -	16:X 18:2–3	16:1–3 18:2–3
PC	16:0, (1–2) 18:(1–2), 3	16:1–3 18:1–3	16:0, (1–2) 18:(1–2), 3	16:1–3 18:1–3
PE	16:0, (1–2) 18:(1–2), 3	16:3 18:1–3	16:0, (1–2) 18:(1–2), 3	16:2–3 18:1–3
PG	16:0, (1) 18:1–3	16:0, $1^{\Delta 3t}$ -	16:0, (1) 18:1–3	16:0, $1^{\Delta 3t}$ -
SQDG	16:0, (1) 18:1–3	16:0, $1^{\Delta 3t}$ -	16:0, (1) 18:1–3	16:0, $1^{\Delta 3t}$ -

Lipid extracts were digested with lipase of *Rhizopus oryzae* to remove fatty acids from the sn-1 position. The lyso-glycerolipids were analyzed by direct infusion tandem mass spectrometry.[1]The fatty acids linked to the sn-1 position have been assumed by the lyso-glycerolipid and glycerolipid composition.

Genome sequencing, assembly and gene annotation

To further investigate light induced differences in the lipid metabolism between the two *Chlorella* species, we draft assembled two comparable Illumina short-read genomes. The assembled genomes of the two *Chlorella* species is distinguishable by their genome characteristics in agreement with the phylogeny (Table 2 and Figure 1). In addition, we generated a more cohesive assembly for *C. sorokiniana* 211-8k using Nanopore technology which is, based on the assembly statistics and BUSCO benchmarking, comparable to the available high quality reference genomes of *C. sorokiniana* UTEX 1602, *C. variabilis* NC64A and *Chlamydomonas reinhardtii* [29,51,52].

Based on the short-read draft assemblies, *C. sorokiniana* 211-8k exhibited an assembled genome size of ∼57 Mb with a GC content of 64% as also found in the recently sequenced *C. sorokiniana* UTEX 1602 (Table 2) [51]. In contrast, *C. vulgaris* 211-11b showed a GC content of 61% and a smaller assembled genome size of 38 Mb, which is in line with the performed *k*-mer based genome size estimates (Supplementary

Table 2 *Chlorella* genome properties

	C. sorokiniana 211-8k	*C. vulgaris* 211-11b	*C. sorokiniana* UTEX 1602 [51]	*C. variabilis* NC64A [52]	*C. reinhardtii* [29]
Total genome size (Mb)	57.2	38.2	59.4	46.2	111.1
GC content (%)	64	61	64	67	64
Number of N's per 100 kbp	9.14	15.51		8546.69	3645.26
Gene count	14,544	11,502	9587	9791	17,741
Avg. gene density (genes/Mb)	252.82	299.48		212.85	159.68
Avg. number of exons per gene	9.78	7.55	14.6	7.3	8.6
Avg. exon length (nt)	146.4	182.5	146	170	260.1
Avg. intron length (nt)	202.97	204.05	231	209	269.9
Avg. coding sequence (%)	44	51	31	29	39

Comparison of sequenced *Chlorella* genomes to the published genomes of *C. sorokiniana* UTEX 1602, *C. reinhardtii* and *C. variabilis* NC64A.

Table S8). Scaffolds of up to 1 Mb were assembled for *C. sorokiniana* 211-8k with a N50 value of 253 kb, while the assembly of *C. vulgaris* 211-11b resulted in a maximum scaffold size of 629 kb and a N50 value of 89 kb.

In addition to the short-read Illumina data we generated ∼50-fold coverage of long Nanopore reads for *C. sorokiniana* 211-8k using an Oxford Nanopore MinION sequencer (Supplementary Table S7). An initial hybrid assembly using SPAdes (v3.9.0) already indicated an improved assembly consisting of 451 contigs with an N50 of 700 kb. Given the sufficient coverage we used Canu [30] for long-read genome assembly with subsequent polishing with Illumina reads using Pilon [53] as this strategy has been shown to provide excellent results for plants [54] (Supplementary Table S9).

The resulting assembly consisted of merely 21 contigs corresponding to a total length of 58 Mb. On both ends of nine contigs, the telomeric repeats (TTTAGG)N and (CCTAAA)N could be identified and additional five contigs contained the respective motif on a single end [55]. Together with a N50 of 4.28 Mb and a largest contig of 6.8 Mb the *C. sorokiniana* 211-8k assembly was in a comparable range to the reference genomes of *C. sorokiniana* UTEX 1602, *C. variabilis* NC64A and *C. reinhardtii* [29,51,52]. Furthermore, the R9.4 1D Nanopore reads were used to estimate 5-methylcytosine (5-mC) modification of CpG sites. Hypomethylated regions, in particular of contig 6 and 7, coincide with a drop in gene density and the lack of contigs from any of the short-read assemblies that were able to span the region (Supplementary Figure S3). Contig 92 and 94 indicate a similar coherence on the ends that do lack a telomeric repeat, suggesting that even the long Nanopore reads were unable to span this complex part of the chromosome. As hypomethylation is known to be associated with centromeric chromatin in higher plants [56] these findings together with the telomeric repeats suggests that the combination of long nanopore reads and short Illumina reads is able to assemble entire chromosome arms for most of the *C. sorokiniana* 211-8k genome.

Completeness was benchmarked using BUSCO with the chlorophyta dataset [43]. After polishing 2055 complete BUSCOs could be found in the assembly of *C. sorokiniana* 211-8k which is comparable to the analyzed reference genome of *C. reinhardtii* (2105) and higher than the reference genome of *C. variabilis* NC64A (1797) (Supplementary Figure S2). Poly(A)+ RNA was sequenced in order to perform gene annotation of the two *Chlorella* species. The gene annotation of *C. vulgaris* 211-11b differed from *C. sorokiniana* in gene counts (11 502vs.14 544) and gene density (299.48 genes/Mb vs. 252.82 genes/Mb) (Table 2). Groups of orthologous genes revealed a close phylogenetic relationship among the *Chlorella* species with 40% (5849) of the groups containing genes conserved in all species (Figure 6). The two analyzed *Chlorella* species showed a higher number of species-specific genes compared to *C. sorokiniana* UTEX 1602 and *C. variabilis* NC64A.

In silico research of glycerolipid metabolism in *Chlorella*

Based on *de novo* sequenced *Chlorella* genomes and predicted *Chlorella* gene models, we reconstructed the glycerolipid metabolism of *Chlorella* by identifying putative orthologs of referenced protein sequences from higher plants (mainly *Arabidopsis thaliana*), algae (mainly *Chlamydomonas reinhardtii*), *Saccharomyces cerevisiae*, cyanobacteria, and some other bacteria [5,44–47,57] (Supplementary Table S2–S5 and Figure 7). Thereby, we identified a highly conserved prokaryotic pathway among the two analyzed *Chlorella* species and higher plants,

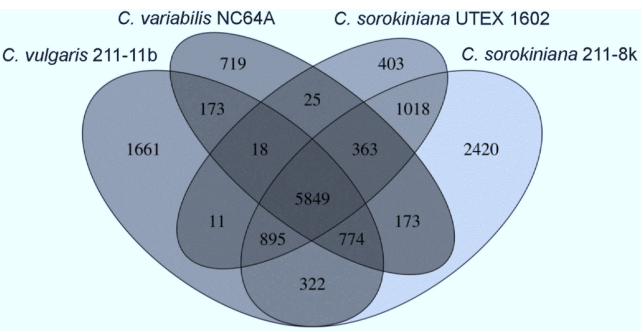

Figure 6. Classification of orthologous groups in different green algae.

Four-way Venn diagram showing the number of conserved or strain-specific orthologous groups identified with OrthoFinder for *C. sorokiniana* 211-8k, *C. vulgaris* 211-11b, *C. sorokiniana* UTEX 1602 and the reference genome *C. variabilis* NC64A.

Biochemical Journal (2020) **477** 2543–2559
https://doi.org/10.1042/BCJ20200160

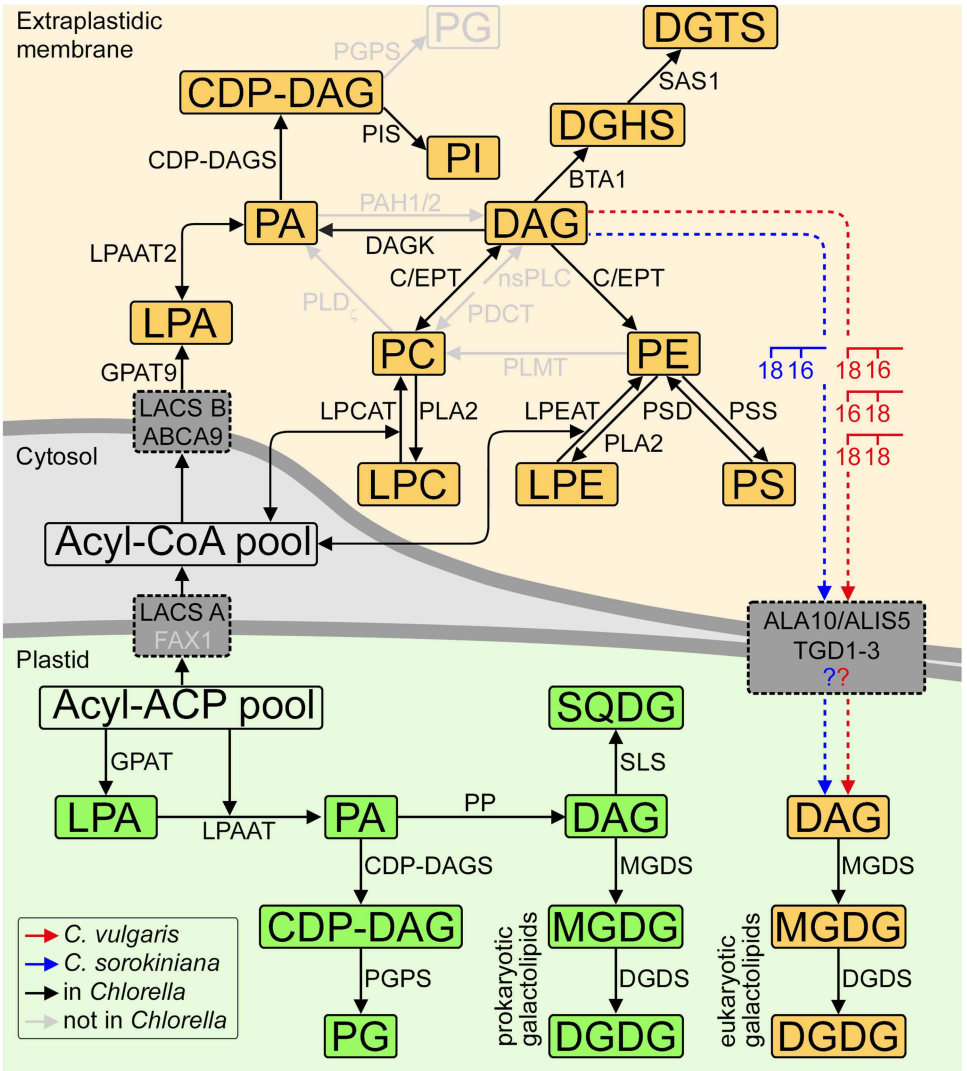

Figure 7. Model of the membrane lipid synthesis in *Chlorella*. Part 1 of 2

The putative lipid synthesis pathway in *Chlorella* is based on our results and numerous previous studies mostly described in Li-Beisson et al. [5]. Within the chloroplast, prokaryotic GPAT mediates the acylation of G3P to LPA. By a second acylation step, catalyzed by LPAAT, LPA is converted to PA, which is either dephosphorylated (PP) to DAG or activated by CDP-DAGS to synthesize CDP-DAG and finally PG is synthesized by PGPS. Inside the chloroplast, DAG represents a branch point between the synthesis of galactolipids and sulfolipids. The glycosylation reaction, catalyzed by MGDS, converts DAG to MGDG, while DGDS transfers a second galactosyl group on MGDG to synthesize DGDG. The final committed step in the biosynthesis of SQDG is catalyzed by SLS, which transfers the anionic sulfoquinovosyl group onto DAG. Synthesis of the so-called eukaryotic lipids starts with the conversion of acyl-ACP to acyl-CoA by LACS and the export to extraplastidic membranes. In green algae, extraplastidic PA is probably synthesized by sequential acylation steps catalyzed by the eukaryotic enzymes GPAT9 and LPAAT2. Additionally, orthologs of *C. reinhardtii* S-adenosylmethionine synthetase (SAS1) and betaine lipid synthase (BTA1), which are involved in DGTS synthesis, were found in *Chlorella.* Since no orthologs of PLDζ, PAH1/2, and PP were found in *Chlorella*, further phospholipid degrading enzymes are probably present in *Chlorella*. The eukaryotic orthologs of CDP-DAGS and PIS utilize PA to synthesize CDP-DAG and finally PI. PE and PC are synthesized by C/EPT which may possess substrate specificity for both CDP-choline and CDP-ethanolamine. PE is converted to PS by PSS, whereas the reverse reaction is catalyzed by PSD. PLA2 is responsible for the release of acyl moieties of PC (PE) to produce LPA (LPE) while the re-acylation to PC (PE) is catalyzed by LPCAT (LPEAT). The acyl editing of PC (PE) results in an exchange of fatty acids and the generation of various PC (PE) species including PC (PE) species with two C-18 acyl chains. DAG species with two C-18 acyl chains are synthesized by the assumed conversion of PC to DAG catalyzed by C/EPT. By a still unknown route, strain specific precursors are probably re-imported to the chloroplast and used for the synthesis of different MGDG and DGDG

Biochemical Journal (2020) **477** 2543–2559
https://doi.org/10.1042/BCJ20200160

Figure 7. Model of the membrane lipid synthesis in *Chlorella*. Part 2 of 2

molecular species. The lipid transport system from the chloroplast to extraplastidic membranes comprises three orthologs of LACS isoforms and ABCA9 while no ortholog of FAX1 was observed in both *Chlorella* strains. The re-import of glycerolipids to the chloroplast is probably mediated by ALA10/ALIS5 and TGD1-3, further TGD orthologs were not found. Detailed information is provided in Supplementary Table S2–S5.

whereas some differences were observed between *Chlorella* and higher plants within the genes coding for enzymes of the eukaryotic pathway [57–59].

In particular, no orthologs of phosphatidylglycerophosphate synthase (PGPS), N-methylphospholipid methyltransferase (PLMT), phospholipase D (PLDζ), phosphatidate phosphatase (PP, PAH1, PAH2), non-specific phospholipase C (nsPLC), and phosphatidylcholinediacylglycerol cholinephosphotransferase (PDCT) were found in any of the *Chlorella* strains. However, some coding sequences for PA, PI, PE, LPC and PC synthesis (diacylglycerol kinase (DAGK), cytidine diphosphate diacylglycerol synthase (CDP-DAGS), phosphatidylinositol synthase (PIS), diacylglycerol choline/ethanolamine phosphotransferase (C/EPT), 1-acylglycerol-3-phosphocholine acyltransferase (LPCAT), 1-acylglycerol-3-phosphatidylethanolamine acyltransferase (LPEAT) [60], phospholipase A2 (PLA2) are present in *Chlorella* [5]. Comparable to other green algae like *C. reinhardtii*, *Chlorella* also possess an ER-localized lysophosphatidic acid acyltransferase (LPAAT2) [12]. Additionally, orthologs of S-adenosylmethionine synthetase (SAS1) and betaine lipid synthase (BTA1), which are involved in DGTS synthesis, were found in *Chlorella* [61].

Both *Chlorella* species possess highly conserved sequences of proteins involved in the export of fatty acids from the chloroplast to the ER which is built up of three different long-chain acyl-CoA synthetases (LACS) and ATP binding cassette transporter A9 (ABCA9) (FAX1 is not present in *Chlorella*) [62,63], possibly converting acyl-ACP to acyl-CoA [64] and generating an acyl-CoA pool outside the chloroplast. Also the re-import machinery from the ER into the chloroplast showed highly conserved protein sequences between both *Chlorella* species. They exhibit the trigalactosyldiacylglycerol ATP binding cassette transporter complex constituted of TGD1, TGD2, and TGD3 whereas TGD4 and TGD5 coding sequences were not found in *Chlorella* [65–67]. Furthermore, both *Chlorella* species possess the phospholipid flippase ALA10 and its interacting subunit ALIS5 which likely transfers PC to the chloroplast at ER-chloroplast contact sides [68]. According to these *in silico* results, both *Chlorella* species are able to synthesize the membrane lipids PA, PG, SQDG, MGDG and DGDG within the chloroplast while the degradation of ER localized phospholipids to DAG (PLDζ, PAH1/2 and nsPLC) is still unclear suggesting the presence of further phospholipid degrading enzymes in green algae. As the re-import machinery of ER-derived precursors for galactolipid synthesis is highly conserved among the two *Chlorella* species, we assume that further lipid transport mechanisms, might facilitate strain specific re-import of ER-derived precursors for the synthesis of eukaryotic galactolipids (Figure 7, blue and red dashed lines).

Discussion

In this study, we focused on high light induced alterations in the glycerolipid metabolism of two *Chlorella* species that strongly differ in their ability to cope with different light conditions. *C. sorokiniana* and *C. vulgaris* differed significantly in their growth characteristics under the tested light conditions.

Likewise, the two species exhibited substantial differences in pigment degradation, oxygen evolution and xanthophylls pool size, which clearly shows that both species evolved different mechanisms to adjust to different light intensities.

To get insights into membrane lipid remodeling under different light conditions, we analyzed membrane glycerolipids and reconstructed the glycerolipid metabolism of both *Chlorella* species. We observed that different light treatment resulted in species specific alterations in the membrane lipid composition with largest differences in the galactolipids MGDG and DGDG. Unlike *C. sorokiniana*, *C. vulgaris* possessed ER-derived galactolipids with C-18 acyl chains at the sn-2 position, which was confirmed by labeling experiments with 18 : 1-CoA and positional analysis. Surprisingly, both species incorporated 16 : 0-CoA into galactolipids indicating that both species utilize ER-derived precursors for the synthesis of galactolipids. Since *C. sorokiniana* and *C. vulgaris* possessed similar PC and PE molecular species, also with C18 acyl-chains at the sn-2 position, we expect that the two *Chlorella* species probably utilize different mechanisms to facilitate selective transport of lipid molecular species from the ER to the chloroplast.

Biochemical Journal (2020) **477** 2543–2559
https://doi.org/10.1042/BCJ20200160

In general, *in silico* analysis showed the presence of highly conserved lipid synthesis pathways among the two species (Figure 7).Also the already characterized TGD transport system and the phospholipid flippase ALA10/ALIS5 are highly conserved among the two *Chlorella* species [65–68]. Certainly, we observed species specific compositions of putative ABC-transporters, but the role of these transporters in the selective transport of ER-derived precursors for galactolipid synthesis needs to be further elucidated. Additionally, *in silico* analysis revealed nearly identical MGDG synthase protein sequences in both *Chlorella* species suggesting similar localization and substrate specificity, which further supports the requirement of different lipid transport mechanisms. Hence, we assume that the species specific shift in the light induced MGDG : DGDG ratio is caused by differences in the relocation of galactolipid precursors from the ER to the chloroplast which makes the desired substrate available. As high light treated *C. vulgaris* changed its MGDG : DGDG ratio from approximately 3 : 1 to 1 : 2, we speculate that this rearrangement is met by the re-import of a different set of ER-derived galactolipid precursors. While both *Chlorella* species possess only one MGDG synthase (MGD1) and DGDG synthase (DGD1), respectively, substrate specificity could also be responsible for the shift of the galactolipid amounts. Possibly, the *Chlorella* DGDG synthase acts preferentially on MGDG with two C-18 acyl chains [69] and, as a consequence, the MGDG:DGDG ratio decreases in high light treated *C. vulgaris* while the MGDG:DGDG ratio of *C. sorokiniana* is less affected because of the exclusive availability of MGDG species with C-16 acyl chains at the sn-2 position. In contrast to light induced changes of the MGDG:DGDG ratio, the observed species specific alterations within the galactolipid molecular species composition is neither explainable by substrate specificity nor by further mechanisms like transcript induction or protein modification. Therefore, we speculate that the adjustment of *Chlorella* cell membranes to different light conditions includes the involvement of so far unknown lipid transport mechanisms.

As the xanthophyll cycle takes place within the thylakoid membranes of chloroplasts [49,70,71], it has been proposed that the solubility of xanthophyll cycle pigments and some enzymes of the xanthophyll cycle depends on the glycerolipid composition [72,73]. Certainly, it is unclear if the observed alterations in lipid classes and lipid molecular species of chloroplast membranes affect the size of the xanthophyll pool or pigment degradation. It is more likely that the availability of several ER-derived precursors enables a species specific membrane adjustment to different light conditions which probably contribute to the maintenance of various photosynthesis and photoprotective processes.

In summary, different light treatments of the two *Chlorella* species, *C. vulgaris* and *C. sorokiniana*, caused species specific shifts within their glycerolipid composition. Although both species are able to re-import ER-derived precursor for galactolipid synthesis into the chloroplast, they strongly differ in their galactolipid molecular species composition supporting the utilization of species specific lipid transport mechanisms. However, its a matter of discussion to what extend these membrane lipid alterations support *Chlorella* cells to acclimate to different light conditions.

Data Availability

The genome data have been deposited at the ENA under accession PRJEB21526.

Competing Interests

The authors declare that there are no competing interests associated with the manuscript.

Funding

This work has been supported by the Federal Ministry of Education and Research (03SF0465) and the Ministry of Innovation, Science and Research within the framework of the NRW-Strategieprojekt BioSC [no. 313/323-400-002 13].

Author Contribution

C.P. designed the project. J.W., J.P. and C.P. performed membrane lipid analysis. J.W. and C.P. carried out growth experiments. C.P. performed pigment analysis. J.W. and J.P. extracted DNA and RNA. A.V. generated short read and long read DNA sequence data, conducted assemblies and performed assembly polishing. *In silico* analysis of lipid pathways were performed by C.P. and J.W. L.A., and H.S. performed RNA-seq data analysis and genome annotation. U.S., B.U. and L.N. analyzed data and provided material. C.P. wrote the manuscript with help from all authors.

Abbreviations

Ant, antheraxanthin; BTA1, betaine lipid synthase; C/EPT, diacylglycerol choline/ethanolamine phosphotransferase; CDP-DAG, cytidine diphosphate diacylglycerol; CDP-DAGS, cytidine diphosphate diacylglycerol synthase; DAG, diacylglycerol; DAGK, diacylglycerol kinase; DES, de-epoxidation state; DGDG, digalactoslydiacylglycerol; DGDS, DGDG synthase; DGHS, diacylglycerylhomoserine; DGTS, diacylglyceryl-N,N,N-trimethylhomoserine; G3P, glycerine-3-phosphate; GPAT, glycerol-3-phosphate acyltransferase; HL, high light; LACS, long chain acyl-CoA synthetase; LL, low light;LPA, lyso-phosphatidic acid; LPAAT, lysophosphatidic acid acyltransferase; LPC, lyso-phosphatidyl choline; LPCAT, 1-acylglycerol-3-phosphocholine acyltransferase; LPEAT, 1-acylglycerol-3-phosphatidylethanolamine acyltransferase; MGDG, monogalactoslydiacylglycerol; MGDS, MGDG synthase; nsPLC, non-specific phospholipase C; PA, phosphatidic acid; PAH1/2, phosphatidate phosphatase; PC, phosphatidylcholine; PDCT, phosphatidylcholinediacylglycerol cholinephosphotransferase; PE, phosphatidyl ethanolamine; PG, phosphatidylglycerol; PGPS, phosphatidylglycerophosphate synthase; PI, phosphatidyl inositol; PIS, phosphatidylinositol synthase; PLA2, phospholipase A2; PLDζ, phospholipase D; PLMT, N-methylphospholipid methyltransferase; PP, phosphatidate phosphatase; PS, phosphatidyl serine; PSD, PS decarboxylase; PSS, PS synthase; SAS1, S-adenosylmethionine synthetase; SLS, sulfolipid synthase; SQDG, sulfoquinovosyldiacylglycerol; TGD1-5, trigalactosyldiacylglycerol ATP binding cassette; Vio, violaxanthin; Zea, zeaxanthin.

References

1 Thompson, G. (1996) Lipids and membrane function in green algae. *Biochim. Biophys. Acta* **1302**, 17–45 https://doi.org/10.1016/0005-2760(96)00045-8
2 Khotimchenko, S.V. and Yakovleva, I.M. (2004) Effect of solar irradiance on lipids of the green alga Ulva fenestrata Postels et Ruprecht. *Bot. Mar.* **47**, 395–401 https://doi.org/10.1515/BOT.2004.050
3 Wacker, A., Piepho, M., Harwood, J.L., Guschina, I.A. and Arts, M.T. (2016) Light-induced changes in fatty acid profiles of specific lipid classes in several freshwater phytoplankton species. *Front. Plant Sci.* **7**, 264 https://doi.org/10.3389/fpls.2016.00264
4 Roughan, P.G. and Slack, C.R. (1982) Cellular organization of glycerolipid metabolism. *Annu. Rev. Plant Physiol.* **1**, 97–132 https://doi.org/10.1146/annurev.pp.33.060182.000525
5 Li-Beisson, Y., Shorrosh, B., Beisson, F., Andersson, M.X., Arondel, V., Bates, P.D. et al. (2013) Acyl-lipid metabolism. *Arabidopsis book* **11**, e0161 https://doi.org/10.1199/tab.0161
6 Xu, C.C., Fan, J.L., Cornish, A.J. and Benning, C. (2008) Lipid trafficking between the endoplasmic reticulum and the plastid in Arabidopsis requires the extraplastidic TGD4 protein. *Plant Cell* **20**, 2190–2204 https://doi.org/10.1105/tpc.108.061176
7 Block, M.A. and Jouhet, J. (2015) Lipid trafficking at endoplasmic reticulum-chloroplast membrane contact sites. *Curr. Opin. Cell Biol.* **35**, 21–29 https://doi.org/10.1016/j.ceb.2015.03.004
8 Nakamura, Y., Koizumib, R., Shuic, S., Shimojimad, M., Wenk, M.R., Ito, T. et al. (2009) Arabidopsis lipins mediate eukaryotic pathway of lipid metabolism and cope critically with phosphate starvation. *Proc. Natl Acad. Sci. U.S.A.* **106**, 20978–20983 https://doi.org/10.1073/pnas.0907173106
9 Frentzen, M., Heinz, E., McKeon, T.A. and Stumpf, P.K. (1983) Specificities and selectivities of glycerol-3-phosphate acyltransferase and monoacylglycerol-3-phosphate acyltransferase from pea and spinach chloroplasts. *Eur. J. Biochem.* **129**, 629–636 https://doi.org/10.1111/j.1432-1033.1983.tb07096.x
10 Heinz, E. and Roughan, G. (1983) Similarities and differences in lipid metabolism of chloroplasts isolated from 18:3 and 16:3 plants. *Plant Physiol.* **72**, 273–279 https://doi.org/10.1104/pp.72.2.273
11 Giroud, C., Gerber, A. and Eichenberger, W. (1988) Lipids of *Chlamydomonas reinhardtii*. Analysis of molecular species and intracellular site(s) of biosynthesis. *Plant Cell Physiol.* **29**, 587–595 https://doi.org/10.1093/oxfordjournals.pcp.a077533
12 Kim, Y., Terng, E.L., Riekhof, W.R., Cahoon, E.B. and Cerutti, H. (2018) Endoplasmic reticulum acyltransferase with prokaryotic substrate preference contributes to triacylglycerol assembly in *Chlamydomonas*. *Proc. Natl Acad. Sci. U.S.A.* **115**, 1652–1657 https://doi.org/10.1073/pnas.1715922115
13 Webb, M.S. and Green, B.R. (1991) Biochemical and biophysical properties of thylakoid acyl lipids. *Biochim. Biophys. Acta* **1060**, 133–158 https://doi.org/10.1016/S0005-2728(09)91002-7
14 Beyerinck, M.W. (1890) Culturversuche mit Zoochlorellen, Lichenengonidien und anderen Algen. *Botanische Zeitung.* **48**, 725–788
15 Sorokin, C. and Krauss, R.W. (1957) The effects of light intensities on the growth rates of green algae. *Plant Physiol.* **33**, 109–113 https://doi.org/10.1104/pp.33.2.109
16 Gorman, D.S. and Levine, R.P. (1965) Cytochrome F and plastocyanin: their sequence in the photosynthetic electron transport chain of *Chlamydomonas reinhardi*. *Proc. Natl Acad. Sci. U.S.A.* **54**, 1665–1669 https://doi.org/10.1073/pnas.54.6.1665
17 Kumar, S., Stecher, G. and Tamura, K. (2015) MEGA7: molecular evolutionary genetics analysis version 7.0 for bigger datasets. *Mol. Biol. Evol.* **33**, 1870–1874 https://doi.org/10.1093/molbev/msw054
18 Bligh, E.G. and Dyer, W.J. (1959) A rapid method of total lipid extraction and purification. *Can. J. Biochem. Physiol.* **37**, 911–917 https://doi.org/10.1139/o59-099
19 Fischer, E. and Speier, A. (1895) Darstellung der ester. *Berichte der deutschen chemischen Gesellschaft* **28**, 3252–3258 https://doi.org/10.1002/cber.189502803176
20 Shiva, S., Sy Vu, H., Roth, M.R., Zhou, Z., Marepally, S.R., Sagar Nune, D. et al. (2013) Lipidomic analysis of plant membrane lipids by direct infusion tandem mass spectrometry. *Methods Mol. Biol.* **1009**, 79–91 https://doi.org/10.1007/978-1-62703-401-2_9

Biochemical Journal (2020) **477** 2543–2559
https://doi.org/10.1042/BCJ20200160

21 Welti, R., Li, W., Li, M., Sang, Y., Biesiada, H., Zhou, H.-E. et al. (2002) Profiling membrane lipids in plant stress responses. Role of phospholipase D alpha in freezing-induced lipid changes in Arabidopsis. *J. Biol. Chem.* **35**, 31994–32002 https://doi.org/10.1074/jbc.M205375200

22 Buseman, C.M., Tamura, P., Sparks, A.A., Baughman, E.J., Maatta, S., Zhao, J. et al. (2006) Wounding stimulates the accumulation of glycerolipids containing oxophytodienoic acid and dinor-oxophytodienoic acid in Arabidopsis leaves. *Plant Phys.* **142**, 28–39 https://doi.org/10.1104/pp.106.082115

23 Devaiah, S.P., Roth, M.R., Baughman, E., Li, M., Tamura, P., Jeannotte, R. et al. (2006) Quantitative profiling of polar glycerolipid species from organs of wild-type Arabidopsis and a phospholipase D alpha1 knockout mutant. *Phytochemistry* **17**, 1907–1924 https://doi.org/10.1016/j.phytochem.2006.06.005

24 Williams, J., Khan, U.M. and Wong, D. (1995) A simple technique for the analysis of positional distribution of fatty acids on di- and triacylglycerols using lipase and phospholipase A2. *J. Lipid Res.* **36**, 1407–1412 PMID:7666017

25 Bolger, A.M., Lohse, M. and Usadel, B. (2014) Trimmomatic: a flexible trimmer for illumina sequence data. *Bioinformatics* **30**, 2114–2120 https://doi.org/10.1093/bioinformatics/btu170

26 Bankevich, A., Nurk, S., Antipov, D., Gurevich, A.A., Dvorkin, M., Kulikov, A.S. et al. (2012) SPAdes: a new genome assembly algorithm and its applications to single-cell sequencing. *J. Comput. Biol.* **19**, 455–477 https://doi.org/10.1089/cmb.2012.0021

27 Camacho, C., Coulouris, G., Avagyan, V., Ma, N., Papadopoulos, J., Bealer, K. et al. (2009) BLAST+: architecture and applications. *BMC Bioinformatics* **10**, 421 https://doi.org/10.1186/1471-2105-10-421

28 Loman, N.J. and Quinlan, A.R. (2014) Poretools: a toolkit for analyzing nanopore sequence data. *Bioinformatics* **30**, 3399–3401 https://doi.org/10.1093/bioinformatics/btu555

29 Koren, S., Walenz, B.P., Berlin, K., Miller, J.R., Bergman, N.H. and Phillippy, A.M. (2017) Canu: scalable and accurate long-read assembly via adaptive k-mer weighting and repeat separation. *Genome Res.* **27**, 722–736 https://doi.org/10.1101/gr.215087.116

30 Walker, B.J., Abeel, T., Shea, T., Priest, M., Abouelliel, A., Sakthikumar, S. et al. (2014) Pilon: an integrated tool for comprehensive microbial variant detection and genome assembly improvement. *PLoS ONE* **9**, e112963 https://doi.org/10.1371/journal.pone.0112963

31 Marçais, G. and Kingsford, C. (2011) A fast, lock-free approach for efficient parallel counting of occurrences of k-mers. *Bioinformatics* **27**, 764–770 https://doi.org/10.1093/bioinformatics/btr011

32 Liu, B., Shi, Y., Yuan, J., Hu, X., Zhang, H., Li, N. et al. (2013) Estimation of genomic characteristics by analyzing k-mer frequency in de novo genome projects. *arXiv* preprint arXiv **1308**, 1–47 https://doi.org/1308.2012

33 Orsini, M., Cusano, R., Costelli, C., Malavasi, V., Concas, A., Angius, A. et al. (2016) Complete genome sequence of chloroplast DNA (cpDNA) of *Chlorella sorokiniana*. Mitochondrial DNA Part A DNA Mapp. *Seq. Anal.* **27**, 838–839 https://doi.org/10.3109/19401736.2014.919466

34 Simpson, J.T., Workman, R.E., Zuzarte, P.C., David, M., Dursi, L.J. and Timp, W. (2017) Detecting DNA cytosine methylation using nanopore sequencing. *Nat. Methods* **14**, 407–410 https://doi.org/10.1038/nmeth.4184

35 Kiełbasa, S.M., Wan, R., Sato, K., Horton, P. and Frith, M.C. (2011) Adaptive seeds tame genomic sequence comparison. *Genome Res.* **21**, 487–493 https://doi.org/10.1101/gr.113985.110

36 Langmead, B. and Salzberg, S. (2012) Fast gapped-read alignment with Bowtie 2. *Nat. Methods* **9**, 357–359 https://doi.org/10.1038/nmeth.1923

37 Kim, D., Pertea, G., Trapnell, C., Pimentel, H., Kelley, R. and Salzberg, S.L. (2013) Tophat2: accurate alignment of transcriptomes in the presence of insertions, deletions and gene fusions. *Genome Biol.* **14**, R36 https://doi.org/10.1186/gb-2013-14-4-r36

38 Van der Auwera, G.A., Carneiro, M.O., Hartl, C., Poplin, R., Del Angel, G., Levy-Moonshine, A. et al. (2013) From FastQ data to high confidence variant calls: the Genome Analysis Toolkit best practices pipeline. *Curr. Protoc. Bioinformatics* **43**, 1–33 https://doi.org/10.1002/0471250953.bi1110s43

39 Smit, A.F.A., Hubley, R. and Green, P. (2013–2015) RepeatMasker Open-4.0, http://www.repeatmasker.org

40 Hoff, K.J., Lange, S., Lomsadze, A., Borodovsky, M. and Stanke, M. (2015) BRAKER1: unsupervised RNA-seq-based genome annotation with geneMark-ET and AUGUSTUS. *Bioinformatics* **32**, 767–769 https://doi.org/10.1093/bioinformatics/btv661

41 Emms, D.M. and Kelly, S. (2015) Orthofinder: solving fundamental biases in whole genome comparisons dramatically improves orthogroup inference accuracy. *Genome Biol.* **6**, 157 https://doi.org/10.1186/s13059-015-0721-2

42 Tomato Genome Consortium. (2012) The tomato genome sequence provides insights into fleshy fruit evolution. *Nature* **30**, 635–641 https://doi.org/10.1038/nature11119

43 Simão, F.A., Waterhouse, R.M., Ioannidis, P., Kriventseva, E.V. and Zdobnov, E.M. (2015) BUSCO: assessing genome assembly and annotation completeness with single-copy orthologs. *Bioinformatics* **31**, 3210–3212 https://doi.org/10.1093/bioinformatics/btv351

44 Li-Beisson, Y., Beisson, F. and Riekhof, W. (2015) Metabolism of acyl-lipids in *Chlamydomonas reinhardtii*. *Plant J.* **82**, 504–522 https://doi.org/10.1111/tpj.12787

45 Berardini, T.Z., Reiser, L., Li, D., Mezheritsky, Y., Muller, R., Strait, E. et al. (2015) The Arabidopsis information resource: making and mining the 'gold standard' annotated reference plant genome. *Genesis* **53**, 474–485 https://doi.org/10.1002/dvg.22877

46 Nakao, M., Okamoto, S., Kohara, M., Fujishiro, T., Fujisawa, T., Sato, S. et al. (2010) Cyanobase: the cyanobacteria genome database update 2010. *Nucleic Acids Res.* **38**, 379–381 https://doi.org/10.1093/nar/gkp915

47 Fahy, E., Subramaniam, S., Murphy, R.C., Nishijima, M., Raetz, C.R., Shimizu, T. et al. (2009) Update of the LIPID MAPS comprehensive classification system for lipids. *J Lipid Res.* **50**, 9–14 https://doi.org/10.1194/jlr.R800095-JLR200

48 Bock, C., Krienitz, L. and Pröschold, T. (2011) Taxonomic reassessment of the genus *Chlorella* (Trebouxiophyceae) using molecular signatures (barcodes), including description of seven new species. *Fottea* **11**, 293–312 https://doi.org/10.5507/fot.2011.028

49 Yamamoto, H.Y., Nakayama, T. and Chichester, C.O. (1962) Studies on the light and dark interconversions of leaf xanthophylls. *Arch. Biochem. Biophys.* **1**, 168–173 https://doi.org/10.1016/0003-9861(62)90060-7

50 Frentzen, M. (2004) Phosphatidylglycerol and sulfoquinovosyldiacylglycerol: anionic membrane lipids and phosphate regulation. *Cur. Opin. Plant Biol.* **3**, 270–276 https://doi.org/10.1016/j.pbi.2004.03.001

51 Arriola, M.B., Velmurugan, N., Zhang, Y., Plunkett, M.H., Hondzo, H. and Barney, B.M. (2018) Genome sequences of *Chlorella sorokiniana* UTEX 1602 and *Micractinium conductrix* SAG 241.80: implications to maltose excretion by a green alga. *Plant J.* **93**, 566–586. Blanc, G., Duncan, G., Agarkova, I., Borodovsky, M., Gurnon, J., Kuo, A., Lindquist, E., Lucas, S., Pangilinan, J., Polle, J., Salamov, A., Terry, A., Yamada, T., Dunigan, D. D., Grigoriev, I. V., Claverie, J.-M., Van Etten, and James L. (2010) The Chlorella variabilis NC64A genome reveals adaptation to photosymbiosis, coevolution with viruses, and cryptic sex. *Plant Cell* 9, 2943–2955 https://doi.org/10.1111/tpj.13789

52 Merchant, S.S., Prochnik, S.E., Vallon, O., Harris, E.H., Karpowicz, S.J., Witman, G.B. et al. (2007) The *Chlamydomonas* genome reveals the evolution of key animal and plant functions. *Science* **318**, 245–250 https://doi.org/10.1126/science.1143609
53 Schmidt, M.H., Vogel, A., Denton, A.K., Istace, B., Wormit, A., van de Geest, H. et al. (2017) De novo assembly of a new *Solanum pennellii* accession using nanopore sequencing. *Plant Cell* **10**, 2336–2348 https://doi.org/10.1105/tpc.17.00521
54 Macas, J., Neumann, P. and Navrátilová, A. (2007) Repetitive DNA in the pea (Pisum sativum L.) genome: comprehensive characterization using 454 sequencing and comparison to soybean and Medicago truncatula. *BMC Genomics* **8**, 427 https://doi.org/10.1186/1471-2164-8-427
55 Zhang, W., Lee, H.R., Koo, D.H. and Jiang, J. (2008) Epigenetic modification of centromeric chromatin: hypomethylation of DNA sequences in the CENH3-associated chromatin in *Arabidopsis thaliana* and maize. *Plant Cell* **20**, 25–34 https://doi.org/10.1105/tpc.107.057083
56 Lamesch, P., Berardini, T.Z., Li, D., Swarbreck, D., Wilks, C., Sasidharan, R. et al. (2012) The Arabidopsis Information Resource (TAIR): improved gene annotation and new tools. *Nucleic Acids Res.* **40**, D1202–D1210 https://doi.org/10.1093/nar/gkr1090
57 Kennedy, E.P. and Weiss, S.B. (1956) The function of cytidine coenzymes in the biosynthesis of phospholipides. *J. Biol. Chem.* **222**, 193–214 PMID:13366993
58 Lands, W.E. (1958) Metabolism of glycerolipides; a comparison of lecithin and triglyceride synthesis. *J. Biol. Chem.* **231**, 883–888 PMID:13539023
59 Wang, L., Shen, W., Kazachkov, M., Chen, G., Chen, Q., Carlsson, A.S. et al. (2012) Metabolic interactions between the Lands cycle and the Kennedy pathway of glycerolipid synthesis in Arabidopsis developing seeds. *Plant Cell* **24**, 4652–4669 https://doi.org/10.1105/tpc.112.104604
60 Jasieniecka-Gazarkiewicz, K., Lager, I., Carlsson, A., Gutbrod, K., Peisker, H., Dörmann, P. et al. (2017) Acyl-CoA:lysophosphatidylethanolamine acyltransferase activity affects growth of Arabidopsis. *Plant Physiol.* **174**, 986–998 https://doi.org/10.1104/pp.17.00391
61 Riekhof, W.R., Andre, C. and Benning, C. (2005) Two enzymes, BtaA and BtaB, are sufficient for betaine lipid biosynthesis in bacteria. *Arch Biochem. Biophys.* **441**, 96–105 https://doi.org/10.1016/j.abb.2005.07.001
62 Kim, S., Yamaoka, Y., Ono, H., Kim, H., Shim, D., Maeshima, M. et al. (2013) AtABCA9 transporter supplies fatty acids for lipid synthesis to the endoplasmic reticulum. *Proc. Natl Acad. Sci. U.S.A.* **110**, 773–778 https://doi.org/10.1073/pnas.1214159110
63 Li, N., Gügel, I.L., Giavalisco, P., Zeisler, V., Schreiber, L., Soll, J. et al. (2015) FAX1, a novel membrane protein mediating plastid fatty acid export. *PLoS Biol.* **13**, e1002053 https://doi.org/10.1371/journal.pbio.1002053
64 Kjellberg, J., Trimborn, M., Andersson, M. and Sandelius, A.S. (2000) Acyl-CoA dependent acylation of phospholipids in the chloroplast envelope. *Biochim. Biophys. Acta* **1485**, 100–110 https://doi.org/10.1016/S1388-1981(00)00040-8
65 Roston, R.L., Gao, J., Murcha, M.W., Whelan, J. and Benning, C. (2012) TGD1, -2, and -3 proteins involved in lipid trafficking form ATP-binding cassette (ABC) transporter with multiple substrate-binding proteins. *J. Biol. Chem.* **25**, 21406–21415 https://doi.org/10.1074/jbc.M112.370213
66 Wang, Z., Xu, C. and Benning, C. (2012) TGD4 involved in endoplasmic reticulum-to-chloroplast lipid trafficking is a phosphatidic acid binding protein. *Plant J.* **4**, 614–623 https://doi.org/10.1111/j.1365-313X.2012.04900.x
67 Fan, J., Zhai, Z., Yan, C. and Xu, C. (2015) Arabidopsis trigalactosyldiacylglycerol5 interacts with TGD1, TGD2, and TGD4 to facilitate lipid ransfer from the endoplasmic reticulum to plastids. *Plant Cell* **10**, 2941–2955 https://doi.org/10.1105/tpc.15.00394
68 Botella, C., Sautron, E., Boudiere, L., Michaud, M., Dubots, E., Yamaryo-Botté, Y. et al. (2016) ALA10, a Phospholipid flippase, controls FAD2/FAD3 desaturation of phosphatidylcholine in the ER and affects chloroplast lipid composition in Arabidopsis thaliana. *Plant Physiol.* **170**, 1300–1314 https://doi.org/10.1104/pp.15.01557
69 Kelly, A.A., Froehlich, J.E. and Dörmann, P. (2003) Disruption of the two digalactosyldiacylglycerol synthase genes DGD1 and DGD2 in Arabidopsis reveals the existence of an additional enzyme of galactolipid synthesis. *Plant Cell* **11**, 2694–2706 https://doi.org/10.1105/tpc.016675
70 Demmig, B., Winter, K., Krüger, A. and Czygan, F.-C. (1987) Photoinhibition and zeaxanthin formation in intact leaves : a possible role of the xanthophyll cycle in the dissipation of excess light energy. *Plant Physiol.* **84**, 218–224 https://doi.org/10.1104/pp.84.2.218
71 Hager, A. and Holocher, K. (1994) Localization of the xanthophyll-cycle enzyme violaxanthin de-epoxidase within the thylakoid lumen and abolition of its mobility by a (light-dependent) pH decrease. *Planta* **192**, 581–589 https://doi.org/10.1007/BF00203597
72 Rockholm, D.C. and Yamamoto, H.Y. (1996) Violaxanthin de-epoxidase (Purification of a 43-kilodalton lumenal protein from lettuce by lipid-affinity precipitaion with monogalactosyldiacylglycerol). *Plant Physiol.* **110**, 697–703 https://doi.org/10.1104/pp.110.2.697
73 Goss, R., Lohr, M., Latowski, D., Grzyb, J., Vieler, A., Wilhelm, C. et al. (2005) Role of hexagonal structure-forming lipids in diadinoxanthin and violaxanthin solubilization and de-epoxidation. *Biochemistry* **10**, 4028–4036 https://doi.org/10.1021/bi047464k